Biogeosciences Discuss., doi:10.5194/bg-2015-622, 2016
Manuscript under review for journal Biogeosciences
Published: 26 January 2016

Biogeosciences Discussions Open Access EGU

Seasonal and diurnal variation in CO fluxes from an agricultural bioenergy crop

M. Pihlatie[1,2], Ü. Rannik[1], S. Haapanala[1], O. Peltola[1], N. Shurpali[3], P. J. Martikainen[3], S. Lind[3], N. Hyvönen[3], P. Virkajärvi[4], M. Zahniser[5], I. Mammarella[1]

[1]Department of Physics, University of Helsinki, P.O. Box 48, FI-00014 University of Helsinki
[2]Department of Food and Environmental Sciences, P.O. Box 56, FI-00014 University of Helsinki
[3]Biogeochemistry research group, Department of Environmental and Biological Sciences, University of Eastern Finland, Yliopistoranta 1D-E, PO Box 1627, Kuopio campus, FI-70211 Finland
[4]Natural Resources Institute Finland, Green technology, Halolantie 31 A, FI-71750 Maaninka Finland
[5]Aerodyne Research, Inc. 45 Manning Road Billerica, MA 01821-3976, USA

Correspondence to: M. Pihlatie (mari.pihlatie@helsinki.fi)

Abstract. Carbon monoxide (CO) is an important reactive trace gas in the atmosphere, while its sources and sinks in the biosphere are only poorly understood. Emissions of CO have been reported from a wide range of soil-plant systems. However, soils are generally considered as a sink of CO due to microbial oxidation processes. We measured CO fluxes by micrometeorological eddy covariance method from a bioenergy crop (reed canary grass) in Eastern Finland over April to November 2011. Continuous flux measurements allowed us to assess the seasonal and diurnal variability, and to compare the CO fluxes to simultaneously measured CO_2, N_2O and heat fluxes as well as relevant meteorological, soil and plant variables in order to investigate factors driving the CO exchange.

The reed canary grass crop was a net source of CO from mid-April to mid-June, and a net sink throughout the rest of the measurement period from July to November 2011. CO fluxes had a distinct diurnal pattern with a net CO uptake in the night and an emission during the daytime with a maximum emission at noon. This pattern was most pronounced during the spring and early summer, during which the most significant relationships were found between daytime CO fluxes and global radiation, net radiation, sensible heat flux, soil heat flux, relative humidity and net ecosystem exchange. The strong positive correlation between CO fluxes and radiation suggests towards abiotic CO production processes, whereas, the relationship of CO fluxes with net ecosystem exchange indicates towards biotic CO formation during crop growth. The study shows a clear need for detailed process-studies accompanied with continuous flux measurements of CO exchange to improve the understanding of the processes associated with CO exchange.

Biogeosciences Discuss., doi:10.5194/bg-2015-622, 2016
Manuscript under review for journal Biogeosciences
Published: 26 January 2016

1 Introduction

Carbon monoxide (CO) is an important reactive trace gas in the atmosphere where it participates in the chemical reactions with hydroxyl radicals (OH), which may lead to the production of a strong greenhouse gas ozone (O_3). The reactions of CO and OH decrease the atmospheric capacity to oxidize atmospheric methane (CH_4), hence indirectly affecting the lifetime of this important greenhouse gas. Although CO itself absorbs only little infrared radiation from the Earth, the cumulative indirect radiative forcing of CO may even be larger than that of a third powerful greenhouse gas nitrous oxide (N_2O) (Myhre et al., 2013). Anthropogenic activities related to burning of fossil fuel and biomass (e.g. forest fires) and photochemical oxidation of CH_4 and non-methane hydrocarbons are the main sources of CO (Duncan et al., 2007), while the reaction with OH is the major sink of CO in the atmosphere (Duncan and Logan, 2008). Soils are globally considered as a sink for CO due to microbial oxidation processes in the soil (Conrad and Seiler, 1982; Potter et al., 1996; Whalen and Reeburgh, 2001; King and Weber, 2007). According to Conrad and Seiler (1980) the soil consumption of CO is a microbial process, it follows first-order kinetics and can take place in both aerobic and anaerobic conditions. In addition to CO consumption, production of CO has been found from a wide range of soils (Moxley and Smith, 1998; Gödde et al., 2000; Varella et al., 2004), plant roots (King and Crosby, 2002; King and Hungria, 2002), living and degrading plant material (Tarr et al., 1995; Schade et al., 1999; Derendorp et al., 2011; Lee et al., 2012) and degrading organic matter (Wilks, 1959; Troxler 1972; Conrad and Seiler 1985b). Emissions of CO from water logged soils have often been attributed to anaerobic production of CH_4 (Funk et al., 1994; Varella et al., 2004); however, most often the CO production has been related to abiotic processes such as thermal or UV-induced degradation of organic matter or plant material (Conrad and Seiler, 1985b; Tarr et al., 1995; Schade et al., 1999; Derendorp et al., 2011; van Asperen et al., 2015; Fraser et al., 2015). Biological processes leading to CO release and the importance of these sources in soils or plants are still poorly understood (Moxley and Smith, 1998; King and Crosby, 2002; Vreman et al., 2011; He and He, 2014).

Most of the reported CO flux measurements are either short-term field experiments from managed tropical, Mediterranean or temperate ecosystems (e.g. Conrad and Seiler 1985a; Moxley and Smith 1998; Schade et al., 1999; Varella et al., 2004; Bruhn et al., 2013; van Asperen et al., 2015), boreal forests and bogs (Funk et al, 1994; Zepp et al., 1997; Kuhlbusch et al., 1998), or laboratory incubations with specific treatments of the soil or plant material (Tarr et al., 1995; King & Crosby 2002; Lee et al., 2012). Reported CO flux rates range from small CO uptake to seasonally and temporally variable emissions with a tendency of CO uptake from natural and dry soils compared to managed or water-logged soils (Conrad et al., 1988; Khalil et al., 1990; Funk et al., 1994; Zepp et al., 1997; Moxley and Smith, 1998; Schade et al., 1999; King, 2000; King & Hungria, 2002; Varella et al., 2004; Galbally et al., 2010). Tall tower (Andreae et al., 2015) and airborne measurements have indicated

Biogeosciences Discuss., doi:10.5194/bg-2015-622, 2016
Manuscript under review for journal Biogeosciences
Published: 26 January 2016

source areas of CO in the Amazon basin (Harriss et al., 1990; Kirchoff and Marinho, 1990) and North American tundra (Gosink and Kelly 1979; Ritter et al., 1992; 1994) suggesting also towards biological CO sources.

To our understanding this is the first study to report long-term and continuous field measurements of CO fluxes (F_{CO}) using micrometeorological eddy covariance (EC) method. We measured CO fluxes above a read canary grass crop over a 9-month snow-free period in 2011 by two parallel laser absorption spectrometers. We compared the CO fluxes with simultaneously measured fluxes of carbon dioxide (CO_2), nitrous oxide (N_2O), heat and energy as well as relevant soil, plant and meteorological variables. This allowed us to analyze the seasonality and diurnal variability in CO fluxes in relation to the synoptic, soil and plant variables as well as the fluxes of CO_2, N_2O, heat and energy.

2 Materials and methods

2.1 Measurement site

The measurements were conducted on a mineral agricultural soil cultivated with reed canary grass (RCG, *Phalaris arundinaceae*, L. cv. Palaton) field located in Maaninka, Eastern Finland (63°9′48.69′′ N, 27° 14′3.29′′ E). The measurements covered a period from snow-melt to the new snowfall, from April to November 2011. Long-term (reference period 1981-2010) annual mean air temperature in the region is 3.2°C and the annual precipitation is 612 mm (Pirinen et al., 2012). RCG is a perennial bioenergy crop. It was fertilized in the beginning of the growing season (23 May) with an N-P-K-S fertilizer containing 76 kg N ha-1 (NO3-N : NH4-N = 47:53). The crop from the previous season was kept at the site over the winter (Burvall, 1997) and was harvested on 28 of April (day 118) (Lind et al., 2015). The spring period (days 118-160) was characterized by fast crop growth with the crop height increasing from about 10 cm in mid-May to 1.7 m in late June, reaching the maximum height of 1.9 m in early July. A 6.3 ha field was cultivated with homogeneous RCG crop. From the sampling location of the EC system the homogenous fetch extended 162, 137, 135 and 178 m to N, E, S and W directions, respectively.

The soil at the site is classified as a Haplic Cambisol/Regosol (Hypereutric, Siltic) (IUSS Working Group WRB, 2007) and the texture of the topsoil (0–28 cm) varied from clay loam to loam based on the US Department of Agriculture (USDA) textural classification system. The soil pH varies from 5.4 to 6.1 within the ploughing layer from the surface to about 30 cm,

Biogeosciences Discuss., doi:10.5194/bg-2015-622, 2016
Manuscript under review for journal Biogeosciences
Published: 26 January 2016

and soil organic matter content between 3 and 11%. The average C/N ratio in the ploughing layer was 14.9 (ranging from 14.1 to 15.7).

We performed footprint analysis in order to identify the source area of the flux measurements. Two limiting cases were analysed: first, a low crop representing the beginning of the campaign, and second, canopy with 1.9 m height representing the RCG canopy after mid-summer. Respectively, the measurement heights 2.2 and 2.4 m were used in the analysis. In the first case we represented the low canopy as the surface with aerodynamic roughness 0.04 m (determined from measurements), in the second case a canopy with leaf area distribution characteristic to RCG crops was represented by a beta distribution. In both cases the sources were assumed at the soil surface. Such an assumption was made due to limited information on source-sink behavior (see Sect. 3 below), and also in order to obtain more conservative footprint estimates. Three stability classes representing unstable (the Obukhov length L = -10 m), near-neutral (L = -100 m) and stable (L = +10 m) conditions were considered. The footprint evaluation was performed by using the Lagrangian stochastic trajectory simulations (e.g. Rannik et al., 2003). The upwind distance contributing 80% of the flux was identified for low/high canopy as follows: 53/23 m, 83/34 m, and 166/60 m for unstable, near-neutral, and stable stratifications, respectively. The conducted footprint analysis reveals that the presence of a canopy significantly reduces footprint extent. Note that the conservative footprint scenario with no canopy is applicable only for a short period of time due to fast canopy growth in the beginning of the campaign (see Fig. 1c).Considering that prevailing wind direction during the measurement period was from SE and SSW directions, and the wind direction interval 110-315° contributed 90% of the half-hour periods used in the analysis, the footprint analysis confirms that the measurements represent the RCG canopy under majority of observation conditions in this study.

2.2 CO flux measurements

The EC measurements were made as a part of the ICOS (Integrated Carbon Observation System) Finland program during April to November 2011. The comparison of four laser-based fast-response gas analyzers to measure nitrous oxide (N_2O) fluxes is presented by Rannik et al. (2015), and the analysis of diurnal variation in N_2O fluxes is presented by Shurpali et al. (submitted). Here we report the results of F_{CO} calculated from the concentration measurements by two continuous-wave quantum cascade lasers: AR-CWQCL (model CW-TILDAS-CS Aerodyne Research Inc., see e.g. Zahniser et al., 2009; Lee et al., 2011) and LGRCW-QCL (model N2O/CO-23d, Los Gatos Research Inc., see e.g. Provencal et al., 2005). The same gas analyzers measured simultaneously the concentrations of N_2O, giving a possibility to compare the N_2O fluxes (F_{N2O}) to F_{CO}.

Biogeosciences Discuss., doi:10.5194/bg-2015-622, 2016
Manuscript under review for journal Biogeosciences
Published: 26 January 2016

The measurement height was 2.2 m until 30 June 2011 when the height was raised to 2.4 m due to the growth of RCG. The gas inlets of the closed-path analyzers were located 10 cm below a sonic anemometer (USA-1, Metek Germany GMBH, respectively) used for measuring turbulent wind components. In addition, CO_2 and H_2O fluxes were measured at the site by an infrared gas analyzer (LI7000 – Li-Cor Inc., Lincoln, NE, USA) connected to a sonic anemometer (R3-50, Gill Solent Ltd., UK). The closed-path gas analyzers were located in an air conditioned cabin at about 15 m east from the air inlet and the anemometers. This wind direction (50-110° sector) was therefore discarded from further analysis due to possible disturbances to flux measurements. Sample lines (PTFE) were shielded and heated slightly above ambient air temperature. Sample lines were 16 meters in length and the sample air flow rates were 13.2 and 11.6 LPM for AR-CWQCL and LGR-CWQCL, respectively (Rannik et al., 2015). The EC measurements were sampled at 10 Hz frequency. A weather station located at the site monitored continuously several meteorological parameters such as air temperature (T_{air}) and relative humidity (RH), precipitation (P_r), wind speed and direction, global (R_{glob}) and net radiation (R_{net}), ground heat flux (G), soil temperature (T_{soil}) and soil water content (SWC). Further details on the EC set-up, instrument specifications and data acquisition, can be found in Rannik et al. (2015) and Lind et al. (2015).

2.3 Data processing and analysis

The EC data processing was performed with post-processing software EddyUH (Mammarella et al., 2016). Filtering to eliminate spikes (Vickers and Mahrt, 1997) was performed according to an approach, where the high frequency EC data were despiked by comparing two adjacent measurements. If the difference between two adjacent concentration measurements of CO was greater than 20 ppb, the following point was replaced with the same value as the previous point.

The spectroscopic correction due to water vapour impact on the absorption line shape was accounted for along with the dilution correction. LGR-CWQCL corrected for the water vapour effect by a built-in module in the LGR data acquisition software; the same applied to AR-CWQCL after software update in July 2011. Prior to this software update, the respective dilution and spectroscopic corrections to AR-CWQCL high-frequency CO mole fraction data were performed during the post-processing phase according to Rannik et al. (2015) with the instrument specific CO spectroscopic coefficient (b=0.28) determined in the field.

Prior to calculating the turbulent fluxes, a 2-D rotation (mean lateral and vertical wind equal to zero) of sonic anemometer wind components was done according to Kaimal and Finnigan (1994) and all variables were linearly detrended. The EC

Biogeosciences Discuss., doi:10.5194/bg-2015-622, 2016
Manuscript under review for journal Biogeosciences
Published: 26 January 2016

fluxes were calculated as 30 min co-variances between the scalars and vertical wind velocity following commonly accepted procedures (e.g. Aubinet et al., 2000). Time lag between the concentration and vertical wind speed measurements induced by the sampling lines was determined by maximizing the covariance. The final processing was, however, done by fixing the time lag to avoid unphysical variation of lag occurring due to random flux errors. Spectral corrections were applied to account for the low and high frequency attenuation of the co-variances. The first order response times of the EC systems were determined to be 0.07 and 0.26 sec for the AR-CWQCL and LGR-CWQCL systems, respectively, following the method by Mammarella et al. (2009). Data quality screening was performed according to Vickers and Mahrt (1997) to ensure exclusion of the system malfunctioning as well as unphysical and/or unusual occasions in measurements. After quality screening, 66.0% of the F_{CO} data (AR-CWQCL) was available, with data coverage of 59.2% during the day-time and 75.9% during the night-time. For details of the data processing and quality screening see Rannik et al. (2015).

To evaluate in detail the seasonal changes in F_{CO} and factors affecting the fluxes the data was divided into six periods (days 110-145 = spring (S), days 146-160 = early summer (ES), days 161-181 = mid-summer (MS), days 205-240 = late summer (LS), days 241-295 = autumn (A), and days 296-325 = late autumn (LA)). The division into these periods was based on seasonal changes in crop growth and development, or changes in F_{CO} and temperature, while the length of the periods were kept as similar in length as possible. Also, F_{CO} were not measured during an instrumental break between days 181 and 204. To compare diurnal changes in the F_{CO}, the data was further divided into daytime (F_{CO_day}) and night-time (F_{CO_night}) data, classified based on solar elevation angle above or below the horizon. Pearson correlations between daytime and nighttime half-hour average fluxes and other measured parameters were determined. Data processing was performed with Matlab version R2014a (The MathWorks, Inc., United States) and the statistical testing with IBM SPSS statistics 23 (IBM Corporation, United States).

3 Results

3.1 Seasonal variation

The RCG field was a net source of CO from mid-April in the spring to the mid-June (days 110-160), after which the site turned to a net sink until the end of the measurement period in November 2011 (days 161-322) (Fig. 1). Cumulative CO flux (cum F_{CO}) curves show that the site was a net sink of CO in the end of the 9-month measurement period. During daytime, the

Biogeosciences Discuss., doi:10.5194/bg-2015-622, 2016
Manuscript under review for journal Biogeosciences
Published: 26 January 2016

net CO fluxes (F_{CO_day}) were positive during the spring and early summer (days 110-160) and again during late summer (days 205-240). These daytime emissions were highest during the spring (Table 1). Night-time CO fluxes were negative (CO uptake) throughout the whole measurement period with a trend of increasing CO consumption towards late autumn (Table 1).

The spring emission period (days 110-145) covered a time (days 110-118) with a standing dry crop from the previous year. The old crop was harvested on 28 of April (day 118), after which the ground consisted mainly of short dead plant material and litter, and a slowly sprouting new RCG. The second emissions period in early summer (days 146-160) was characterized by fast growing RCG crop, high and fertilizer-induced N_2O emissions (Shurpali et al., in review), increasing air and soil temperatures, growing leaf area and increasing NEE (Fig. 1). After the crop had reached its maximum height of 1.9 m in mid-June (around day 160), the site started to act as a net sink of CO, followed by a period of net daytime emissions during late summer in July-August (days 205-240). The autumn was characterized by decreasing F_{CO} and slowly dropping temperatures, decreasing radiation intensity, and decreasing photosynthesis activity of the crop (less negative NEE) (Fig. 1).

3.2 Diurnal variation

The F_{CO} had a distinct diurnal pattern with a near constant CO uptake in the night-time and an emission during the day time with maximum emissions at noon (Fig. 2). This pattern was most pronounced during the spring, days 110-145, when the maximum daytime CO emissions reached 2.7 nmol m-2 s-1 (Fig. 2). The net F_{CO} was positive (emission) during the spring and early summer, after which the night-time uptake dominated making the site as a net sink of CO (Fig. 2, Table 1.). Nighttime F_{CO} show nearly constant uptake of CO over the whole measurement period (Fig. 2, Table 1.). Assuming a constant CO uptake also during daytime, gross daytime CO emission (gross F_{CO}) were estimated by subtracting the nighttime F_{CO} from the daytime F_{CO}. The gross F_{CO} show that the site emitted CO throughout the whole measurement period with the highest emissions during the spring and late summer (Table 1). During mid-summer and autumn the gross F_{CO} were markedly smaller, and less than half of the emissions during the spring. The smallest gross F_{CO} were measured in late autumn (Table 1).

The diurnal F_{CO} over the six periods followed closely the daily pattern of R_{glob} (Fig. 3). However, the highest radiation intensity was reached during the early summer (days 145-160), while the maximum F_{CO} were observed during the spring (Figs. 2 and 3).

Biogeosciences Discuss., doi:10.5194/bg-2015-622, 2016
Manuscript under review for journal Biogeosciences
Published: 26 January 2016

The diurnal variation in NEE was very small during the spring (days 110-145) (Fig. 4). A rapid increase in LAI and GAI at around day 150 (Fig. 1d) lead to an increase in CO_2 uptake during daytime, which is seen in a distinct diurnal pattern with negative NEE during daytime and a small positive NEE during night-time (Fig. 4). Maximum NEE values were reached during mid-June (days 161-181) after which the NEE slowly decreased and the CO_2 uptake disappeared by mid-October (day 290) (Figs 1 and 4).

3.3 Driving factors for CO fluxes

The most pronounced relationships between F_{CO} and other measured scalars were found during the two emission periods in the spring and early summer (Table 2, Figure 5). Furthermore, the strongest correlations were found during the spring between F_{CO_day} and R_{glob} ($r=0.760$, $p<0.001$), R_{net} ($r=0.760$, $p<0.001$), H ($r=0.729$, $p<0.001$) and G ($r=0.575$, $p<0.001$). These positive correlations remained significant but became weaker during the early summer (Table 2, Figure 5). Strong negative correlations were found during the spring between F_{CO_day} and RH ($r=-0.537$, $p<0.001$), and during the early summer with NEE ($r=-0.469$, $p<0.001$), while the correlation between daytime F_{CO} and F_{N2O} or ecosystem respiration (RESP) were very weak throughout the 9-month measurement period (Table 2).

Night-time F_{CO} correlated very weakly ($r<0.200$) with H, LE and G during the spring and early summer, and with NEE, RESP, LE, T_{air}, G, T_{soil} and precipitation during the late summer and autumn (data not shown).

4 Discussion

Based on the 9-month EC flux measurements at the RCG crop, we demonstrate that the EC method is suitable for measuring CO fluxes (F_{CO}) from an agricultural bioenergy crop. We show that the soil-plant system acted as a net source of CO during the spring and early summer and a net sink of CO over the late summer and autumn, and that the F_{CO} had a clear diurnal variability. To our knowledge, similar long-term and continuous F_{CO} data series measured by the EC method over any ecosystem type does not exist, and hence this study is unique in bringing new insight to the understanding of short-term diurnal and long-term seasonal F_{CO} dynamics at ecosystem-level. Combining the continuous F_{CO} data with simultaneously measured CO_2, N_2O and energy fluxes as well as meteorological and soil variables allowed us to distinguish driving variables of the F_{CO}, and demonstrate the suitability of the EC method to analyze ecosystem-level CO exchange dynamics.

Biogeosciences Discuss., doi:10.5194/bg-2015-622, 2016
Manuscript under review for journal Biogeosciences
Published: 26 January 2016

The F_{CO} rates from the RCG crop in this study were in the same range as those reported from different natural and managed ecosystems across the different climatic regions (Table 3). There is, however, a tendency of higher CO uptake from boreal forests and grasslands (Zepp et al., 1997; King, 2000; Constant et al., 2008) compared to croplands, which are often reported to emit CO (King, 2000; Galbally et al., 2010, Table 3). The reported CO flux measurements from different climatic regions are, however, mostly short-term studies with measurement periods covering from few weeks to one year. Also, as the majority of the reported fluxes are conducted by manually operated chambers and the measurements have been restricted mostly to daytime. This may bias the flux estimates if the CO fluxes follow a strong diurnal cycle, as found in our study and as reported in many environments (e.g. Varella et al., 2004; Galbally et al., 2010; van Asperen et al., 2015).

Cumulative CO fluxes (cum F_{CO}) over the whole measurement period showed that the RCG crop was a net sink of CO. This cum F_{CO} estimation may be biased due to the instrumental break during July (days 181-205), during which we do not have an estimate of the CO fluxes. Also, due to the fact that the data processing removed more daytime values (40.8% removed) compared to night-time data (24.1% removed), the night-time CO uptake is weighing more in the cumulative flux estimation, potentially leading to smaller fluxes than estimated based on an equal number of flux data from daytime and night-time. Although, acting as a net sink, the F_{CO} had a clear diurnal pattern with CO emissions during daytime and CO uptake during night. This source-sink pattern existed over the whole measurement period with decreasing emissions towards the end of the autumn.

The existing literature suggests that the net CO exchange involves simultaneous production and consumption processes, both of which occur in a variety of soil-plant systems under aerobic and anaerobic conditions. While the consumption of atmospheric CO seems to be clearly a microbial process in the soil (Conrad & Seiler, 1980), the production of CO has been mostly linked with photodegradation or thermal degradation of soils, organic matter and vegetation (Conrad and Seiler 1985a; 1985b; Moxley and Smith 1998; Lee et al., 2012; Bruhn et al., 2013; Fraser et al., 2015) or to a minor extent to anaerobic microbial activity in wet soils (Funk et al., 1994).

Based on the seasonal variation, we could clearly divide the F_{CO} to a distinct emission period and an uptake period. During the "emission" period (days 110-160), the soil-plant system was a strong source of CO during day-time and a constant sink during night time. Furthermore, the emission period was divided into a spring emission period (days 110-145) and an early summer period (days 146-160), which differed from each other based on the relationships with other measured variables such as radiation and NEE. The highest CO emissions were observed during the spring emission period in April to early May when the air and soil temperatures were rather low, crop was not yet actively photosynthesizing (low LAI, low NEE), while radiation was already rather high. During this spring period, the strongest correlations were observed between daytime F_{CO}

Biogeosciences Discuss., doi:10.5194/bg-2015-622, 2016
Manuscript under review for journal Biogeosciences
Published: 26 January 2016

and solar radiation (Rglob, Rn), sensible heat flux and soil heat flux, all indicating a close connection between F_{CO} and radiation and heat transfer. Schade et al. (1999) found a strong influence of incident radiation intensity and temperature on CO fluxes in South African savanna, and that the thermally induced CO emissions were lower than photochemically induced. In their measurements the photochemical CO production was described by a 2nd order polynomial in light intensity and exhibited a hysteresis effect. They also demonstrated that UV irradiation caused the most of the CO emissions whereas visible light lead to up to 40% of the total emissions.

Similar to our findings from the emission period, soils from boreal to tropical regions have been found to have a clear diurnal pattern with emissions in the noon and uptake during the night (Conrad & Seiler, 1985a; Kisselle et al., 2002; Constant et al., 2008; van Asperen et al., 2015). In the studies of Conrad and Seiler (1985a) and van Asperen et al. (2015) the dominating CO production process was thermal chemical decomposition of soil organic matter or plant litter, while the CO consumption was due to microbial activity in the soil. Conrad and Seiler (1985a) claimed that the thermal degradation had a high activation energy, hence following the daily pattern of soil temperature, while the microbial consumption of CO showed only a small activation energy and also a small diurnal rhythm. In our study, the net CO uptake during night-time indicates that there is a near-constant microbial sink of atmospheric CO, as suggested also by Conrad and Seiler (1985a). During daytime, this CO consumption most probably exists, and may even be increased due to temperature dependency. However, we expect that the CO consumption is overruled by daytime CO production, creating the observed diurnal pattern. Similarly, Bruhn et al. (2013) showed with an enclosure method that a temperate grass field was a sink of CO when the measurements were conducted in dark, while CO was emitted under daylight. They suggested that radiation, and especially UV radiation, was the key component in CO production, as the CO emission in UV-excluded sunlight was about half of the CO emission in daylight (Bruhn et al., 2013).

The strength of the EC method is to provide a spatially integrated fluxes of the target compounds over an undisturbed and homogenous ecosystem. This provides a unique tool to understand short-term temporal variability in the fluxes and to link the flux dynamics to other simultaneously measured environmental variables. Due to the fact that the EC method measures net fluxes, we cannot directly separate between different processes, such as CO production and consumption. However, based on process understanding and our data, we made an assumption that most of the CO production takes place during daytime and that the microbial CO consumption is constant throughout the day. After these assumptions, we could divide the data into daytime and night-time periods, which we consider are dominated by either production or consumption processes. This furthermore allowed us to interpret the results of the correlation analysis between F_{CO} and other measured scalars and environmental variables. Based on the high correlations between daytime F_{CO} and Rglob (and other radiation components),

Biogeosciences Discuss., doi:10.5194/bg-2015-622, 2016
Manuscript under review for journal Biogeosciences
Published: 26 January 2016

we expect that radiation is the main driver of CO emissions during the spring and early summer. Correlation between F_{CO} and soil heat flux (G), and that between F_{CO} and T_{air} indicate that also thermal degradation plays an important role in daytime CO formation. As the correlation between F_{CO} and T_{soil} was poor, the T_{soil} at the depth of 2.5 cm does not seem to reflect the location of thermal degradation. However, a better correlation between F_{CO} and T_{air} indicates that most likely majority of thermal degradation takes place on the soil surface or in (dead) organic matter on top of the soil where it is the warmest during the day, and where temperatures are directly influenced by radiation. A close look at the diurnal pattern of F_{CO} during the autumn and summer days during the time of sunrise or sunset reveals that photodegradation is clearly not the sole source of CO at the site, giving support towards thermal degradation or biological processes. In Figures 2 and 3 (days 296-325) we can see that the F_{CO} starts to increase before the sun rise at around 9 am. Similarly, during the summer days (days 205-240), the F_{CO} in the afternoon continues to decrease after the sun set at around 20 pm. These observations suggests towards thermally induced F_{CO}, which may exist throughout the day.

As the F_{CO} measurements commenced soon after the snow melt at the site, the elevated spring-time CO emissions probably resulted from the degradation of the readily available last year's crop and litter, which has been shown to be a significant source of CO (King et al., 2012; Lee et al., 2012). Decreasing amount of this readily degradable organic matter would also partly explain the decreasing trend in CO emissions during spring and early summer. Based on the poor correlation between daytime F_{CO} and ecosystem respiration (RESP), we suggest that the CO emissions are not driven by soil microbial activity, which is known to be temperature dependent. Also, the poor correlation between daytime F_{CO} and F_{N2O} suggests that CO fluxes are neither connected to N_2O forming or consuming nitrogen cycling processes. Based on these arguments, we suggest that during the spring emission period (days 110-145) most of the produced CO originates through abiotic processes, primarily via photodegradation of dead and senescent plant material and top-soil organic matter.

Factors supporting the CO production through photodegradation include high C to N ratio of the plant material, presence of oxygen, greater solar radiation exposure (no shading), and litter area to mass ratio (Tarr et al., 1995; King et al., 2012; Lee et al., 2012). At our site, especially during the spring, dry dead plant matter from the previous year's crop has a high C to N ratio (mean ±stdev: 66±6.3) and it was well exposed to radiation as there was no shading from the growing crop, all supporting for potentially optimal conditions for photodegradation.

At the RCG crop, the early summer emission period in May - June (days 146-160) coincides with the steepest slope in CO_2 uptake (more negative NEE), supporting the findings of Bruhn et al. (2013) and Fraser et al. (2015) that CO can be emitted not only from dead plant matter but also from living green leaves. Similarly, we measured daytime CO emissions during July-August (days 205-240) when the crop had reached maximum height and was photosynthesizing actively, and when the

Biogeosciences Discuss., doi:10.5194/bg-2015-622, 2016
Manuscript under review for journal Biogeosciences
Published: 26 January 2016

dead plant litter on the ground was fully shaded from the sun by up to 1.9 m high crop and maximum LAI of 5.3 m2 m-2. The fact that the CO emissions during the summer periods were lower than those during the spring are in line with the suggestion that the CO emissions from photodegradation generally decrease with increasing leaf area index (King et al., 2012), and that the CO photoproduction efficiency is lower for living plants compared to senescent or dead vegetation (Tarr et al., 1995; Erickson et al., 2015).

Although we cannot separate between biotic and abiotic CO formation at the bioenergy crop, our findings of daytime net CO emissions also during the peak LAI in July and maximum NEE, indicate that some CO may also be formed via plant physiological processes. In fact, different abiotic stresses seem to induce CO production in plants (He and He, 2014) and biological CO formation has been observed via heme oxidation (Engel et al., 1972; Vreman et al., 2011), aromatic amino acid degradation (Hino and Tauchi, 1987), and lipid peroxidation reactions (Wolff and Bidlack, 1976). Carbon monoxide is also suggested to play an important role in cell-cell signalling (Ingi et al., 1996; He and He, 2014) and regulation of root growth (Xuan et al., 2007). The importance of these biological CO forming processes to the global CO budget is, however, still largely unknown (King and Crosby, 2002). An aspect demonstrating the lack of understanding in sink-source dynamics of CO, King and Crosby (2002) showed that plant roots are capable of producing CO, and that this CO source can be as high as the current global estimate of CO sink by soils.

In our study, the fact that the strong correlations during the emission period between F_{CO} and global radiation, sensible heat flux and soil heat flux disappeared during the late summer and autumn indicates that the driving factors for CO exchange during the spring and early summer were different to those during the late-summer and autumn. We expect that when radiation as the driving factor for CO emissions decreased during late summer, the near-constant soil CO consumption started to dominate, which is seen in the decreasing diurnal cycle in the F_{CO}. We also suggest that the source of CO may also have changed from the dead and senescent plant litter in the spring to the green living vegetation during mid-summer. Both of these have been identified as sources of CO via abiotic photodegradation, however, the smaller emissions of CO from the living plants are explained by a lower production efficiency compared to senescent or dead vegetation (Erickson et al., 2015). Still the role of biological CO forming processes remain unresolved and call for further process-studies.

This is the first study to apply EC based techniques to measure long-term variation in F_{CO} at any ecosystem type in the world. In addition to the long-term seasonal variability in the F_{CO}, we were able to identify the driving variables and processes at ecosystem level, findings that have previously been shown with plot scale chamber measurements or in the laboratory. The high diurnal and seasonal variability over the 9-month measurement period shows that there is an urgent

Biogeosciences Discuss., doi:10.5194/bg-2015-622, 2016
Manuscript under review for journal Biogeosciences
Published: 26 January 2016

need for continuous and long-term assessment of F_{CO}. The limitations of the EC method, such as inability to separate between CO production and consumption processes, naturally increase uncertainties in the interpretation of the results. However, despite these limitations, the data allowed us to distinguish between the daytime and night-time processes involved and to link the diurnal and seasonal variability to abiotic and biotic processes. Also, the EC method has clear advantages over the traditional enclosure methods such as measuring non-disturbed ecosystem fluxes and avoiding surface reactions with measurement material, both supporting the application of the EC method to measure F_{CO} in different ecosystems.

5 Conclusions

Long-term and continuous EC based measurements of F_{CO} over an arable read canary grass showed clear seasonal variation with net emissions during the spring and early summer, and net uptake of CO during the late summer and autumn. Daytime emissions of CO and night-time uptake of CO demonstrate the dynamic nature of parallel consumption and production processes. Based on daytime and night-time separation of F_{CO}, and correlation analysis between F_{CO} and radiation, T_{soil}, T_{air}, heat fluxes (H, LE), NEE and ecosystem respiration, the daytime CO emissions were suggested to be driven mainly by radiation and indirect effects of radiation such as heat fluxes. Abiotic photodegradation of plant material and soil organic matter was considered as the main CO forming process during daytime, whereas the night-time CO uptake was expected to be dominated by microbial consumption of CO. This study demonstrates the applicability of the EC method in CO flux measurements at ecosystem scale, and shows the potential in linking the short-term F_{CO} dynamics to its environmental drivers. In order to fully understand the source-sink dynamics and processes of CO exchange, continuous and long-term F_{CO} measurements in combination with process-based studies are urgently needed.

Acknowledgements

This work was supported by the Academy of Finland (project nos. 118780, 127456, 1118615 and 263858, 294088, 288494). ICOS (271878), ICOS-Finland (281255) and ICOS-ERIC (281250), DEFROST Nordic Centre of Excellence and InGOS EU are gratefully acknowledged for funding this work. This work was also supported by institutional research funding (IUT20-11) of the Estonian Ministry of Education and Research. The UEF part of the research work was supported by the funding from the UEF infrastructure funding, Academy of Finland FidiPro programme (PIs – Profs Pertti Martikainen and Seppo

Kellomäki) and the Ministry of Agriculture and Forestry, Finland and MTT Agrifood Research Finland (MTT) strategic funding (project no. 21030028).

References

Andreae, M. O., Acevedo, O. C., Araùjo, A., Artaxo, P., Barbosa, C. G. G., Barbosa, H. M. J., Brito, J., Carbone, S., Chi, X., Cintra, B. B. L., da Silva, N. F., Dias, N. L., Dias-Júnior, C. Q., Ditas, F., Ditz, R., Godoi, A. F. L., Godoi, R. H. M., Heimann, M., Hoffmann, T., Kesselmeier, J., Könemann, T., Krüger, M. L., Lavric, J. V., Manzi, A. O., Lopes, A. P., Martins, D. L., Mikhailov, E. F., Moran-Zuloaga, D., Nelson, B. W., Nölscher, A. C., Santos Nogueira, D., Piedade, M. T. F., Pöhlker, C., Pöschl, U., Quesada, C. A., Rizzo, L. V., Ro, C.-U., Ruckteschler, N., Sá, L. D. A., de Oliveira Sá, M., Sales, C. B., dos Santos, R. M. N., Saturno, J., Schöngart, J., Sörgel, M., de Souza, C. M., de Souza, R. A. F., Su, H., Targhetta, N., Tóta, J., Trebs, I., Trumbore, S., van Eijck, A., Walter, D., Wang, Z., Weber, B., Williams, J., Winderlich, J., Wittmann, F., Wolff, S., and Yáñez-Serrano, A. M.: The Amazon Tall Tower Observatory (ATTO): overview of pilot measurements on ecosystem ecology, meteorology, trace gases, and aerosols. Atmos. Chem. Phys., 15, 10723–10776, doi:10.5194/acp-15-10723-2015, 2015.

van Asperen, H., Warneke, T., Sabbatini, S., Nicolini, G., Papale, D., and Notholt J.: The role of photo- and thermal degradation for CO_2 and CO fluxes in an arid ecosystem. Biogeosciences, 12, 4161–4174, 2015.

Aubinet, M., Grelle, A., Ibrom, A., Rannik, Ü., Moncrieff, J., Foken, T., Kowalski, A.S., Martin, P.H., Berbigier, P., Bernhofer, Ch., Clement, R., Elbers, J., Granier, A., Grünwald, T., Morgenstern, K., Pilegaard K., Rebmann C., Snijders W., Valentini R. and Vesala, T.: Estimates of the annual net carbon and water exchange of European forests: the EUROFLUX methodology, Advances Ecol, Res., 30, 113-175, 2000.

Bruhn, D., Albert, K. R., Mikkelsen, T. N. and Ambus, P.: UV-induced carbon monoxide emission from living vegetation. Biogeosciences, 10, 7877–7882. doi:10.5194/bg-10-7877-2013, 2013.

Burvall, J.: Influence of harvest time and soil type on fuel quality in reed canary grass (Phalaris arundinacea L.), Biomass Bioenerg., 12, 149–154, 1997.

Conrad, R., and Seiler, W.: Role of microorganisms in the consumption and production of atmospheric carbon monoxide by soils. Applied and Environmental Microbiology, 40(3), 437-445, 1980.

Conrad, R., and Seiler, W.: Arid soils as a source of atmospheric carbon monoxide. Geophysical Research Letters, 9(12), 1353-1356, 1982.

Conrad, R., and Seiler, W.: Influence of temperature, moisture and organic carbon on the flux of H2 and CO between soil and atmosphere. Field studies in subtropical regions. J. Geophys. Res, 90, 5699-5709, 1985a.

Conrad, R., and Seiler, W.: Characteristics of abiological carbon monoxide formation from soil organic matter, humic acids, and phenolic compounds. Environ. Sci. Technol., 19(12), 1165-1169, 1985b.

Constant, P., Poissant, L., and Villemur, R.: Annual hydrogen, carbon monoxide and carbon dioxide concentrations and surface to air exchanges in a rural area (Quebec, Canada). Atmospheric Environ. 42, 5090–5100, 2008.

Derendorp, L., Quist, J.B., Holzinger, R., Röckmann, T.: Emissions of H2 and CO from leaf litter of *Sequoiadendron giganteum* and their dependence on UV radiation and temperature. Atmospheric Environ., 45, 7520-7524, 2011.

Duncan, B.N., and Logan, J.A.: Model analysis of the factors regulating the trends and variability of carbon monoxide between 1988 and 1997. Atmos. Chem. Phys., 8, 7389-7403, doi:10.5194/acp-8-7389-2008, 2008.

Duncan, B.N., Logan, J.A., Bey, I., Megretskaia, I.A., Yantosca, R.M., Novelli, P.C., Jones, N.B., and Rinsland, C.P.: Global budget of CO, 1988–1997: Source estimates and validation with a global model, J. Geophys. Res., 112, D22301, doi:10.1029/2007jd008459, 2007.

Engel, R.R., Matsen, J.M., Cpahpamn, S.S., and Schwartz, S.: Carbon monoxide production from heme compounds by bacteria. J. Bacteriology, 112(3), 1310-1315, 1972.

Erickson III, D.J., Sulzberger, B., Zepp, R.G. and Austin, A.T.: Effects of stratospheric ozone depletion, solar UV radiation, and climate change on biogeochemical cycling: interactions and feedbacks. Photochem. Photobiol. Sci., 2015, 14, 127-148, 2015.

Fraser, W.T., Blei, E., Fry, S.C., Newman, M.F., Reay, D.S., Smith, K.A., and McLeod, A.R.: Emission of methane, carbon monoxide, carbon dioxide and short-chain hydrocarbons from vegetation foliage under ultraviolet irradiation. Plant, Cell and Environment, 38, 980–989, 2015.

Gödde, M., Meuser, K., and Conrad, R.: Hydrogen consumption and carbon monoxide production in soils with different properties. Biol. Fertil. Soils, 32, 129-134, 2000.

He, H., and He. L.: The role of carbon monoxide signaling in the responses of plants to abiotic stresses. Nitric Oxide, 42, 40-43, 2014.

Hino, S., and Tauchi, H.: Production of carbon monoxide from aromatic amino acids by *Morganella morganii*. Archives for Microbiology, 148, 167-171, 1987.

Ingi, T., Cheng, J., and Ronnett, G.V.: Carbon monoxide: an endogenous modulator of the nitric oxide-cyclic GMP signalling system. Neuron, 16, 835-842, 1996.

IUSS Working Group WRB: World Reference Base for Soil Resources 2006, first update 2007, World Soil Resources Reports No.103, FAO, Rome, 128 pp., 2007.

Kaimal, J. C. and Finnigan, J. J.: Atmospheric Boundary Layer Flows. Their Structure and Measurement, Oxford University Press, New York, 1994.

King, G. M.: Impacts of land use on atmospheric carbon monoxide consumption by soils. Global Biogeochemical Cycles, 14, 1161-1172, 2000.

King, G. M., and Crosby, H.: Impacts of plant roots on soil CO cycling and soil-atmosphere CO exchange. Global Change Biology, 8, 1085-1093, 2002.

King, G. M., and Hungria, M.: Soil-Atmosphere CO Exchanges and Microbial Biogechemistry of CO Transformations in a Brazilian Agricultural Ecosystem. Applied and Environmental Microbiology, 68(9), 4480-4485, 2002.

King, G. M., and Weber, C. F.: Distribution, diversity and ecology of aerobic CO-oxidizing bacteria. Nature Reviews, Microbiology, 5, 107-118, 2007.

Kisselle, K. W., Zepp, R. G., Burke, R. A., Pinto, A. S., Bustamante, M. M. C., Opsahl, S., Varella, R. F. and Viana, L. T.: Seasonal soil fluxes of carbon monoxide in burned and unburned Brazilian savannas, J. Geophys. Res., 107(D20), 8051, doi:10.1029/2001JD000638, 2002.

Kuhlbusch, T.A.J., Zepp, R.G., Miller, W.L., and Burke, R.A.: Carbon monoxide fluxes of different soil layers in upland Canadian boreal forests. Tellus, 50B, 353-365, 1998.

Lind, S.E., Shurpali, N.J., Peltola, O., Mammarella, I., Hyvönen, N., Maljanen, M., Räty, M., Virkajärvi, P., and P. J. Martikainen: Carbon dioxide exchange of a perennial bioenergy crop cultivation on a mineral soil. Biogeosciences Discuss., 12, 16673–16708, 2015.

Mammarella, I., Launiainen, S., Grönholm, T., Keronen, P., Pumpanen, J., Rannik, Ü., and Vesala, T.: Relative Humidity Effect on the High-Frequency Attenuation of Water Vapor Flux Measured by a Closed-Path Eddy Covariance System, Journal of Atmospheric and Oceanic Technology, 26, 1856-1866, 2009

Mammarella, I., Peltola, O., Nordbo, A., Järvi, L., and Rannik, Ü.: EddyUH: an advanced software package for eddy covariance flux calculation for a wide range of instrumentation and ecosystems, Atmos. Meas. Tech. Discuss., doi:10.5194/amt-2015-323, in review, 2016.Moxley, J.M., and Smith, K.A.: Carbon monoxide production and emission by some Scottish soils. Tellus, 50B, 151-162, 1998.

Myhre, G., D. Shindell, F.-M. Bréon, W. Collins, J. Fuglestvedt, J. Huang, D. Koch, J.-F. Lamarque, D. Lee, B. Mendoza, T. Nakajima, A. Robock, G. Stephens, T. Takemura and H. Zhang.: Anthropogenic and Natural Radiative Forcing. In: Climate Change 2013: The Physical Science Basis. Contribution of Working Group I to the Fifth Assessment Report of the Intergovernmental Panel on Climate Change [Stocker, T.F., D. Qin, G.-K. Plattner, M. Tignor, S.K. Allen, J. Boschung, A. Nauels, Y. Xia, V. Bex and P.M. Midgley (eds.)]. Cambridge University Press, Cambridge, United Kingdom and New York, NY, USA.

Pirinen, P., Simola, H., Aalto, J., Kaukoranta, J., Karlsson, P., and Ruuhela, R.: Tilastoja Suomen ilmastosta 1981–2010, Finnish Meteorological Institute, Helsinki, 2012.

Potter, C.S., Klooster, S.A., and Chatfield, R.B.: Consumption and production of carbon monoxide in soils: a global model analysis of spatial and seasonal variation. Chemosphere, 33(6), 1175-1193, 1996.

Provencal, R., Gupta, M., Owano, T. G., Baer, D. S., Ricci, K. N., O'Keefe, A., and Podolske, J. R.: Cavity-enhanced quantumcascade laser-based instrument for carbon monoxide measurements, Appl. Optics, 44, 6712–6717, 2005.

Rannik, Ü., Markkanen, T., Raittila, J., Hari, P., and Vesala, T.: Turbulence statistics inside and over forest: influence on footprint prediction, Boundary-Layer Meteorol., 109(2), 163-189, 2013.

Rannik, Ü., Haapanala, S., Shurpali, N. J., Mammarella, I., Lind, S., Hyvönen, N., Peltola, O., Zahniser, M., Martikainen, P. J., and T. Vesala: Intercomparison of fast response commercial gas analysers for nitrous oxide flux measurements under field conditions. Biogeosciences 12, 415–432, 2015.

Schade, G.W., Hofmann, R.-M., and Crutzen, P.J.: CO emissions from degrading plant matter. Tellus 51B, 889-908, 1999.

Tarr, M.A., Miller, W.L., and Zepp, R.G.: Direct carbon monoxide photoproduction from plant matter. J. Geophys. Res., 100, D6, 11403-11413, 1995.

Varella, R.F., Bustamante, M.M.C., Pinto, A.S., Kisselle, K.W., Santos, R.V., Burke, R.A., Zepp, R.G., and Viana, L.T.: Soil fluxes of CO_2, CO, NO and N_2O from an old pasture and from native savanna in Brazil. Ecological Applications, 14(4), Supplement, S221-S231, 2004.

Vickers, D. and Mahrt, L.: Quality control and flux sampling problems for tower and aircraft data, J. Atmos. Ocean. Tech., 14, 512–526, 1997.

Vreman, H.J., Wong, R.J., Stevenson, D.K.: Quantitating carbon monoxide production from heme by vascular plant preparations in vitro. Plant Physiology and Biochemistry, 49, 61-68, 2011.

Wolff, D.G., Bidlack, W.R.: The formation of carbon monoxide during peroxidation of microsomal lipids. Biochemical and Biophysical Research Communications, 2, 15-18, 1976.

Biogeosciences Discuss., doi:10.5194/bg-2015-622, 2016
Manuscript under review for journal Biogeosciences
Published: 26 January 2016

Xuan, W., Huang, L, Li, M., Huang, B., Xu, S., Liu, H., Gao, Y., Shen, W.: Induction of growth elongation in wheat root segments by heme molecules: a regulatory role of carbon monoxide in plants? Plant Growth Regul. 52, 41-51, 2007.

Zepp, R. G., Miller, W. L., Tarr, M. A., Burke, R. A.: Soil-atmosphere fluxes of carbon monoxide during early stages of postfire succession in upland Canadian boreal forests. J. Geophys. Res. 102(D24), 29301-29311, 1997

Biogeosciences Discuss., doi:10.5194/bg-2015-622, 2016
Manuscript under review for journal Biogeosciences
Published: 26 January 2016

Table 1. Mean, median and 25-75th percentiles of the CO fluxes (F_{CO}, nmol m^{-2} s^{-1}) measured in a read canary grass (RCG) crop at Maaninka. Mean daytime (sun elevation, $h_{sun} > 0$) and nighttime ($h_{sun}<0$) fluxes are calculated during six measurement periods (S = spring, ES = early summer, MS = mid-summer, LS = late summer, A = autumn, LA = late autumn), and over the full measurement period from April to November 2011. Gross CO fluxes (gross F_{CO_day}) refer to the difference between daytime fluxes (F_{CO_day}) and nighttime fluxes (F_{CO_night}).

	F_{CO_day}				F_{CO_night}				net F_{CO}				gross F_{CO_day}			
Period, days	mean	median	25th-75th percentile		mean	median	25th-75th percentile		mean	median	25th-75th percentile		mean	median	25th-75th percentile	
S, 110-145	0.97	0.68	-0.15	2.00	-0.64	-0.56	-0.97	-0.20	0.41	0.09	-0.57	1.28	1.61	1.24	0.83	2.20
ES, 146-160	0.24	0.08	-0.29	0.57	-0.67	-0.49	-0.72	-0.33	0.03	-0.10	-0.45	0.43	0.91	0.57	0.43	0.91
MS, 161-181	-0.07	-0.08	-0.40	0.24	-0.67	-0.52	-0.86	-0.22	-0.22	-0.18	-0.55	0.16	0.59	0.45	0.46	0.46
LS, 205-240	0.36	0.30	-0.07	0.87	-0.76	-0.49	-0.96	-0.19	-0.09	-0.04	-0.53	0.49	1.12	0.79	0.89	1.07
A, 241-295	-0.12	-0.18	-0.48	0.13	-0.66	-0.61	-0.90	-0.32	-0.44	-0.44	-0.77	-0.10	0.54	0.42	0.41	0.45
LA, 296-325	-0.62	-0.59	-0.94	-0.26	-1.05	-1.01	-1.37	-0.65	-0.92	-0.89	-1.25	-0.49	0.42	0.42	0.43	0.39
All, 110-325	0.21	0.01	-0.41	0.55	-0.77	-0.66	-1.06	-0.33	-0.25	-0.34	-0.79	0.17	0.98	0.68	0.65	0.88

Biogeosciences Discuss., doi:10.5194/bg-2015-622, 2016
Manuscript under review for journal Biogeosciences
Published: 26 January 2016

Table 2. Pearson correlation matrix for half-hour daytime CO fluxes (F_{CO_day}) during four periods (two emission periods: days 110-145 and days 146-160, and two uptake periods: days 161-240, and days 241-325) at the reed canary grass crop in Maaninka. NEE = net ecosystem exchange, RESP = ecosystem respiration, F_{N2O} = N_2O flux, H = sensible heat flux, LE = latent heat flux, T_{air} = air temperature, R_{glob} = global radiation, R_{net} = net radiation, G = soil heat flux, T_{soil} = soil temperature at 2.5 cm, SWC = soil water content at 2.5 cm.

	F_{CO_day} days 110-145		n	F_{CO_day} days 146-160		n	F_{CO_day} days 161-240		n	F_{CO_day} days 241-325		n
NEE	-0.188	**	711	-0.469	**	510	-0.327	**	896	-0.292	**	1110
RESP	0.015		711	0.274	**	510	0.271	**	896	0.291	**	1110
F_{N2O}	-0.219	**	669	0.000		453	-0.163	**	878	-0.045		1109
H	0.729	**	711	0.329	**	510	0.331	**	896	0.103	**	1111
LE	0.402	**	418	0.398	**	401	0.485	**	517	0.367	**	735
RH	-0.537	**	711	-0.176	**	510	-0.295	**	896	-0.161	**	1111
T_{air}	0.425	**	711	0.344	**	510	0.397	**	896	0.307	**	1111
R_{glob}	0.760	**	711	0.498	**	510	0.435	**	896	0.311	**	1111
R_{net}	0.760	**	711	0.515	**	510	0.445	**	896	0.318	**	1111
G	0.575	**	711	0.473	**	510	0.401	**	896	0.239	**	1111
T_{soil}	0.191	**	711	0.282	**	510	0.355	**	896	0.289	**	1111
SWC	-0.099	**	711	0.033		510	0.191	**	896	-0.128	**	1111

**Correlation is significant at the 0.01 level (2-tailed).
*Correlation is significant at the 0.05 level (2-tailed).

Biogeosciences Discuss., doi:10.5194/bg-2015-622, 2016
Manuscript under review for journal Biogeosciences
Published: 26 January 2016

Table 3. Reported CO fluxes measured in the field by chamber (transparent or dark), micrometeorological flux gradient or eddy covariance methods.

Reference	Ecosystem, climate, country	Measurement method	Data period	F_{CO} (nmol m^{-2} s^{-1})
Zepp et al., 1997	Black spruce forest, boreal, Manitoba, Canada	Chambers, transparent	3 months	-1.06
Zepp et al., 1997	Jack pine forest, boreal, Manitoba, Canada	Chambers, transparent	3 months	-0.58
King, 2000	Pine forest, Northeast, Walpole, Maine, USA	Chambers, dark	1.3 years	1.12
King, 2000	Mixed hardwood-coniferous forest, Walpole, Maine, USA	Chambers, dark	1.3 years	0.62
King, 2000	Pine forest, Griffin, Georgia, USA	Chambers, dark	1 year	-0.21
King, 2000	Pine forest, Tifton, Georgia, USA	Chambers, dark	1 year	-0.95
Kuhlbusch et al., 1998	Black spruce, boreal, Manitoba, Canada	Chambers, dark	1 year	-1.11
Galbally et al. 2010	Mallee, Eucalyptus sp. Ecosystem, tropical, Australia	Chambers, transparent	1 year, every second month	0.61
Varella et al., 2004	Natural cerrado, tropical, Brazil	Chambers, transparent	1.5 years	1.91
Varella et al., 2004	Pasture (*Brachiaria brizantha*), tropical, Brazil	Chambers, transparent	1.5 years	1.20
Constant et al., 2008	Grassland, boreal, Quebec, Canada	Flux gradient	1 year	-2.11
Bruhn et al., 2013	Grassland, temperate, Denmark	Chambers, dark	2 months	-0.78
Bruhn et al., 2013	Grassland, temperate, Denmark	Chambers, transparent	2 months	0.36
van Asperen et al., 2015	Grassland, Mediterranean, Italy	Chambers, transparent	5 weeks, summer	0.35
van Asperen et al., 2015	Grassland, Mediterranean, Italy	Flux gradient	1 month, summer	1.74
King, 2000	Cropland, corn, Walpole, Maine, USA	Chambers, dark	1.3 years	2.19
King, 2000	Cropland, sorghum/wheat, Griffin, Georgia, USA	Chambers, dark	1 year	1.16
King, 2000	Cropland, cotton/peanuts/winter wheat, Tifton, Georgia, USA	Chambers, dark	1 year	1.03
Galbally et al. 2010	Cropland, wheat, tropical, Australia	Chambers, transparent	1 year, every second month	0.98
this study	Cropland, reed canary grass, boreal, Finland	Eddy covariance	9 months	-0.25

Biogeosciences Discuss., doi:10.5194/bg-2015-622, 2016
Manuscript under review for journal Biogeosciences
Published: 26 January 2016

Figure captions

Figure 1. (a) Daily mean air and soil temperatures, (b) global radiation sum (R_{glob}), (c) daily precipitation sum (Pr) and soil water content (SWC), (d) weekly leaf area index (LAI) (blue) and green area index (GAI) (green), (e) net ecosystem exchange (NEE), and (f) cumulative CO fluxes (cum F_{CO}; blue and green) and daytime mean CO fluxes (F_{CO_day}; red) over the 9-month measurement period in a reed canary grass crop. Measurement periods (S = spring, ES = early summer, MS = mid-summer, LS = late summer, A = autumn, LA = late autumn) are separated by solid lines.

Figure 2. Diurnal cycle of half-hour average CO fluxes (F_{CO}, nmol m^{-2} s^{-1}) from the reed canary grass crop from six distinct periods during the April to November 2011 measurement campaign. The vertical bars indicate ±1 standard deviation of the fluxes.

Figure 3. Diurnal cycle of half-hour average global radiation (R_{glob}, W m^{-2}) the reed canary grass crop from six distinct periods during the April to November 2011 measurement campaign. The vertical bars indicate ±1 standard deviation of the fluxes.

Figure 4. Diurnal cycle of half-hour average net ecosystem exchange (NEE, µmol m^{-2} s^{-1}) from the reed canary grass crop from six distinct periods during the April to November 2011 measurement campaign. The vertical bars indicate ±1 standard deviation of the fluxes.

Figure 5. Daytime half-hour average CO fluxes (F_{CO}) against global radiation (R_{glob}), sensible heat flux (H) and net ecosystem exchange (NEE) measured over two emission periods (days 110-145, days 146-160) at the reed canary grass crop in Maaninka. The bin averages with ±1 standard deviation are presented in black.

Biogeosciences Discuss., doi:10.5194/bg-2015-622, 2016
Manuscript under review for journal Biogeosciences
Published: 26 January 2016

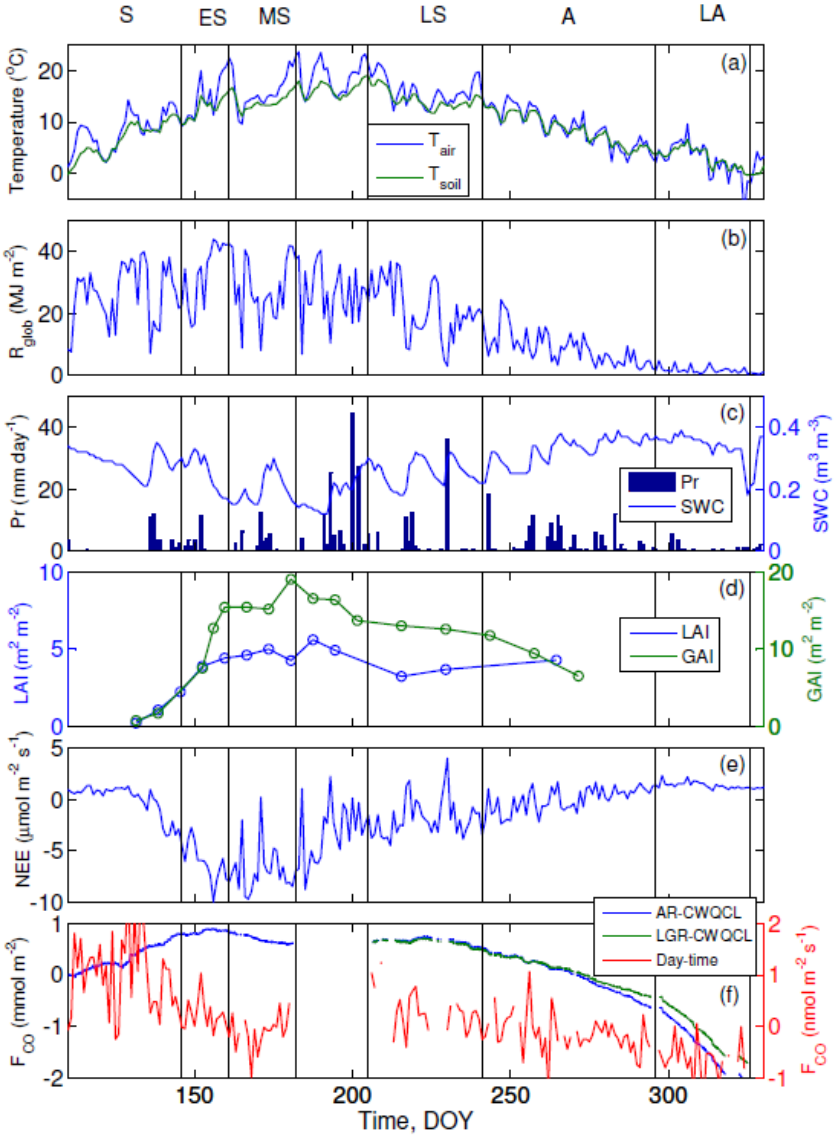

Figure 1. (a) Daily mean air and soil temperatures, (b) global radiation sum (R_{glob}), (c) daily precipitation sum (Pr) and soil water content (SWC), (d) weekly leaf area index (LAI) (blue) and green area index (GAI) (green), (e) net ecosystem exchange (NEE), and (f) cumulative CO fluxes (cum F_{CO}; blue and green) and daytime mean CO fluxes (F_{CO_day}; red) over the 9-month measurement period in a reed canary grass crop. Measurement periods (S = spring, ES = early summer, MS = mid-summer, LS = late summer, A = autumn, LA = late autumn) are separated by solid lines.

Biogeosciences Discuss., doi:10.5194/bg-2015-622, 2016
Manuscript under review for journal Biogeosciences
Published: 26 January 2016

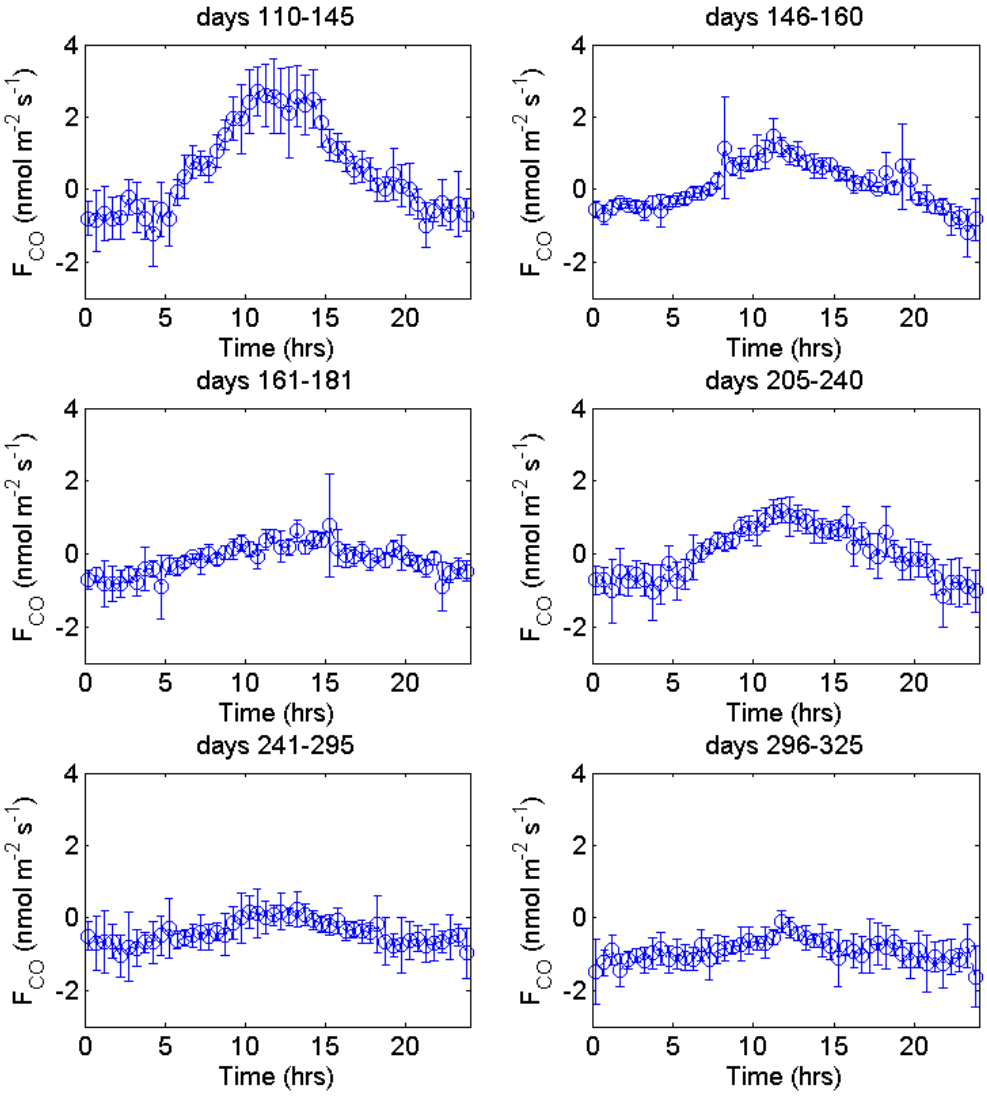

Figure 2. Diurnal cycle of half-hour average CO fluxes (F_{CO}, nmol m^{-2} s^{-1}) from the reed canary grass crop from six distinct periods during the April to November 2011 measurement campaign. The vertical bars indicate ±1 standard deviation of the fluxes.

Biogeosciences Discuss., doi:10.5194/bg-2015-622, 2016
Manuscript under review for journal Biogeosciences
Published: 26 January 2016

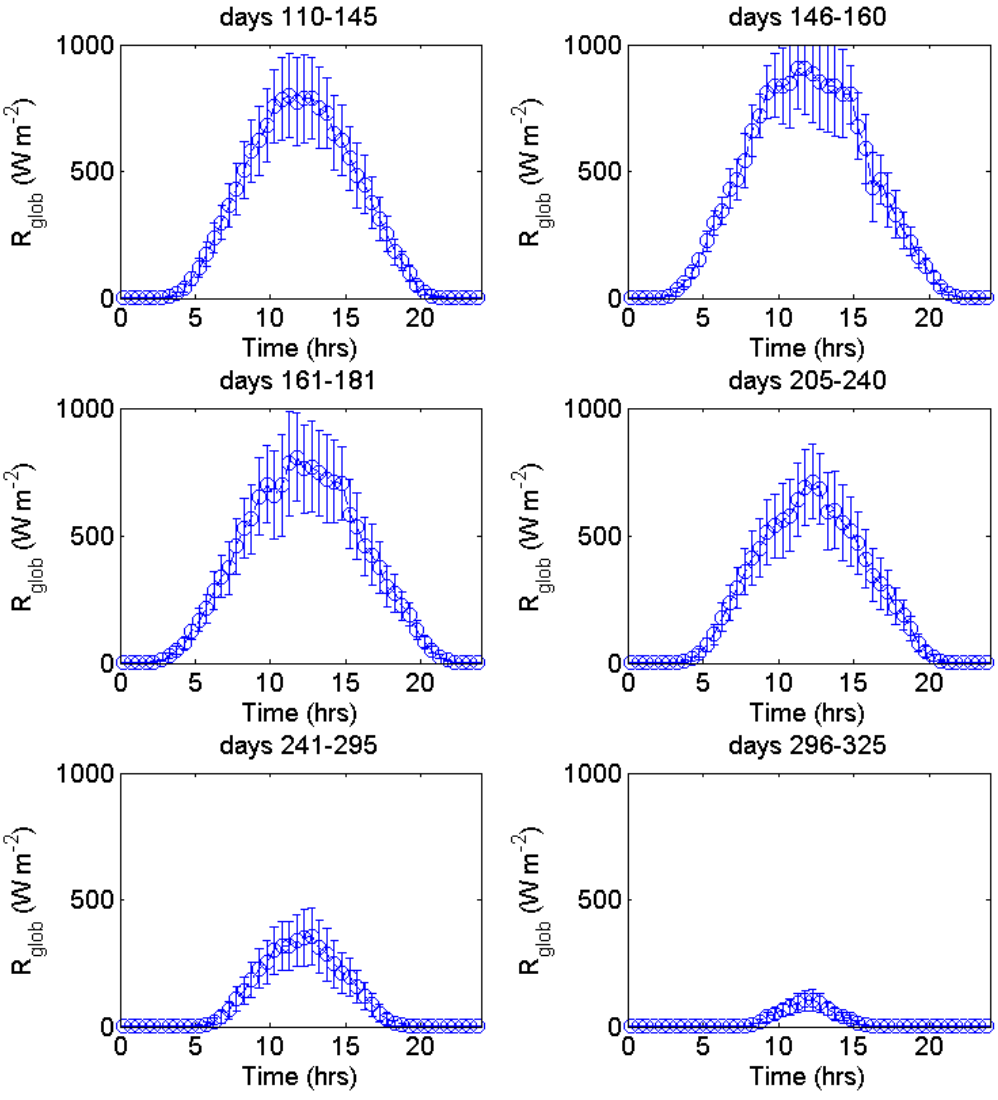

Figure 3. Diurnal cycle of half-hour average global radiation (R_{glob}, W m^{-2}) the reed canary grass crop from six distinct periods during the April to November 2011 measurement campaign. The vertical bars indicate ±1 standard deviation of the fluxes.

Biogeosciences Discuss., doi:10.5194/bg-2015-622, 2016
Manuscript under review for journal Biogeosciences
Published: 26 January 2016

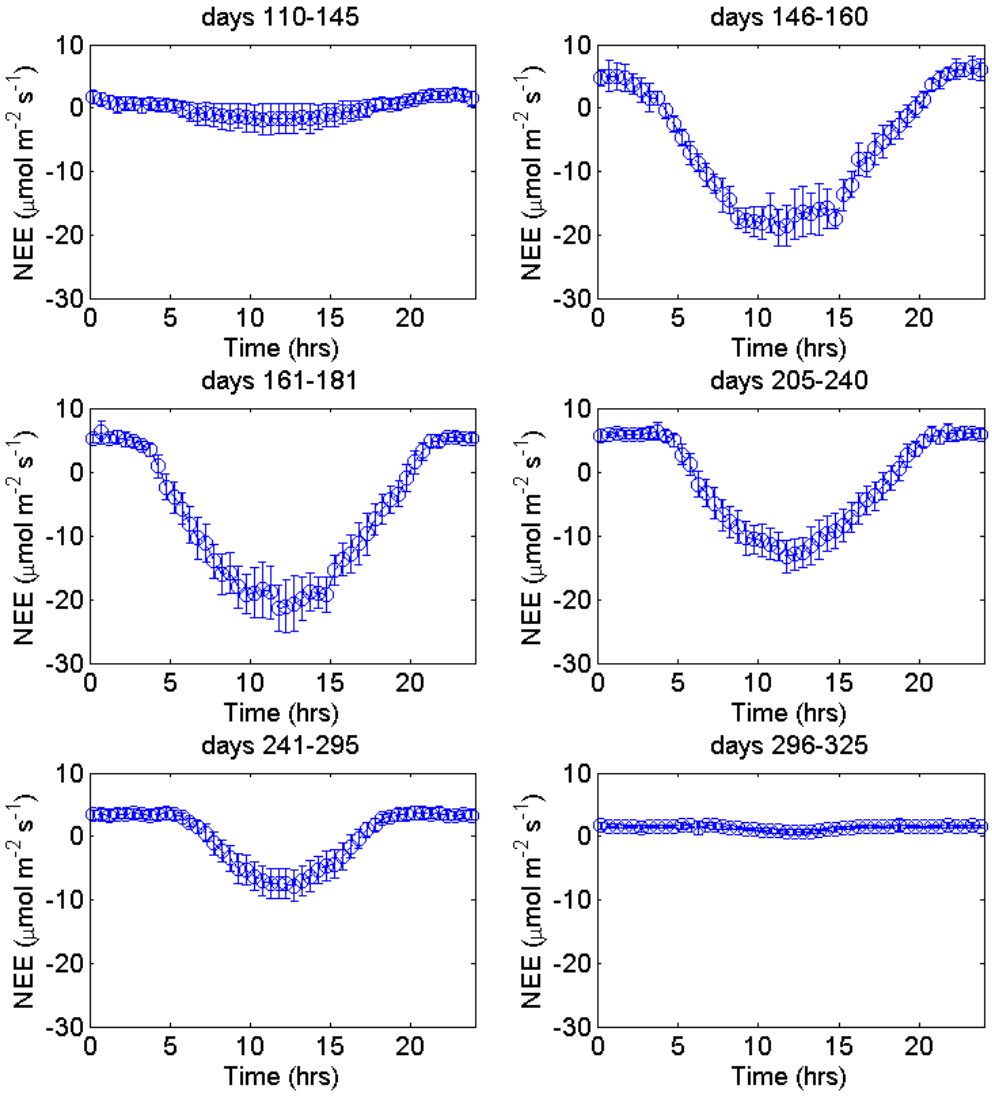

Figure 4. Diurnal cycle of half-hour average net ecosystem exchange (NEE, μmol m^{-2} s^{-1}) from the reed canary grass crop from six distinct periods during the April to November 2011 measurement campaign. The vertical bars indicate ±1 standard deviation of the fluxes.

Biogeosciences Discuss., doi:10.5194/bg-2015-622, 2016
Manuscript under review for journal Biogeosciences
Published: 26 January 2016

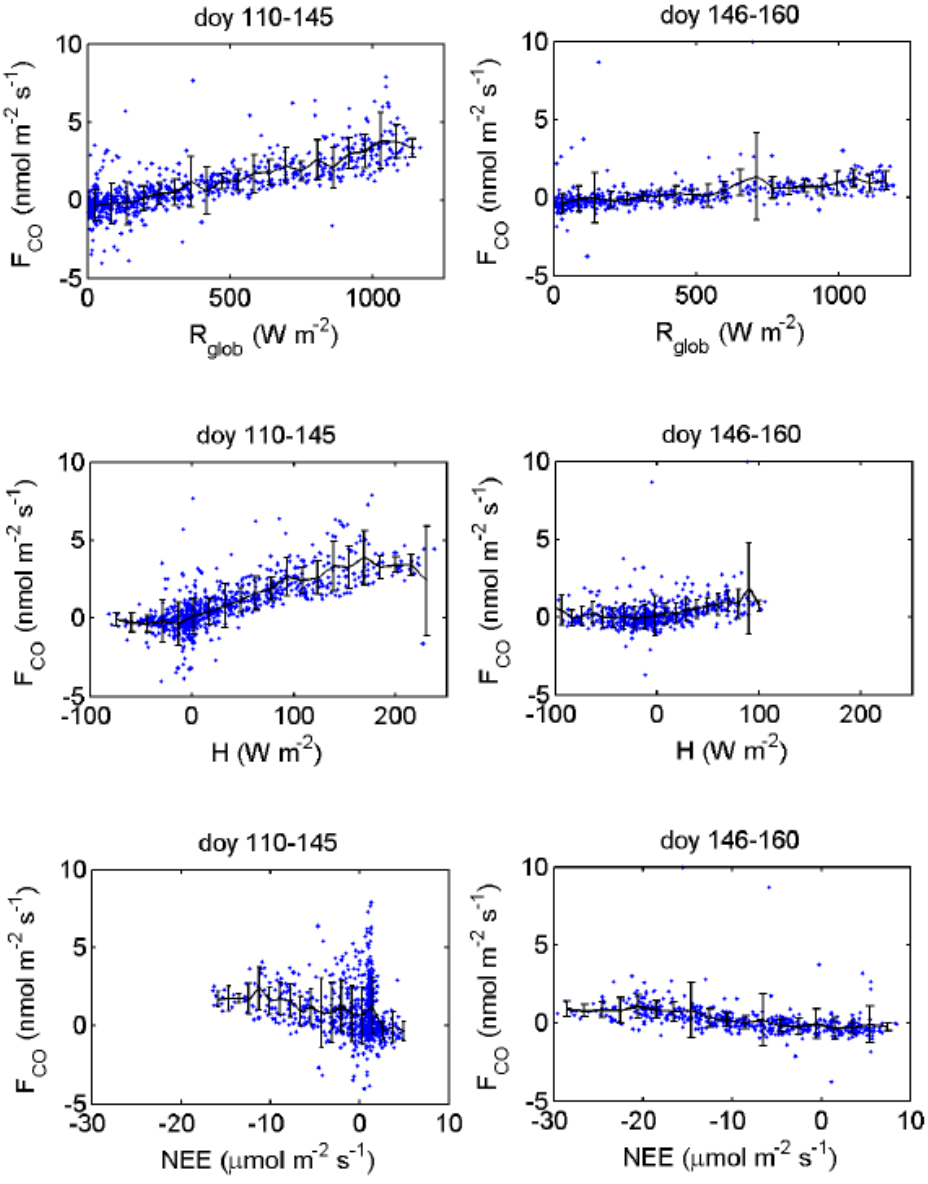

Figure 5. Daytime half-hour average CO fluxes (F_{CO}) against global radiation (R_{glob}), sensible heat flux (H) and net ecosystem exchange (NEE) measured over two emission periods (days 110-145, days 146-160) at the reed canary grass crop in Maaninka. The bin averages with ±1 standard deviation are presented in black.